

1

| REPORT DOCUMENTATION PAGE   |       |   |  | Form Approved<br>OMB No. 0704-0188   |                                 |
|---|-------|---|--|--|---------------------------------|
| 1a. REPORT SECURITY CLASSIFICATION<br>Unclassified  |       |   | 1b. RESTRICTIVE MARKINGS   |  |                                 |
| 2. AUTHOR(OR ORGANIZATION) REPORT NUMBER<br>AD-A213 113   |       |   | 3. DISTRIBUTION/AVAILABILITY OF REPORT<br>Approved for public release;<br>distribution is unlimited. |  |                                 |
| 4. PERFORMING ORGANIZATION NAME(S) AND ADDRESS(ES)<br>Aerodynamics Branch<br>Aeromechanics Division<br>Air Force Armament Laboratory<br>Eglin AFB FL 32542-5434   |       |   | 5. MONITORING ORGANIZATION REPORT NUMBER(S)<br>AFATL-TP-89-16  |  |                                 |
| 6a. NAME OF PERFORMING ORGANIZATION<br>Aerodynamics Branch<br>Aeromechanics Division  |       | 6b. OFFICE SYMBOL<br>(If applicable)<br>AFATL/FXA |  | 7a. NAME OF MONITORING ORGANIZATION<br>Aerodynamics Branch<br>Aeromechanics Division |                                 |
| 6c. ADDRESS (City, State, and ZIP Code)<br>Air Force Armament Laboratory<br>Eglin AFB FL 32542-5434   |       |   | 7b. ADDRESS (City, State, and ZIP Code)<br>Air Force Armament Laboratory<br>Eglin AFB FL 32542-5434  |  |                                 |
| 8a. NAME OF FUNDING/SPONSORING ORGANIZATION<br>Aeromechanics Division   |       | 8b. OFFICE SYMBOL<br>(If applicable)<br>AFATL/FXA |  | 9. PROCUREMENT INSTRUMENT IDENTIFICATION NUMBER                                      |                                 |
| 8c. ADDRESS (City, State, and ZIP Code)<br>Air Force Armament Laboratory<br>Eglin AFB FL 32542-5434   |       |   | 10. SOURCE OF FUNDING NUMBERS  |  |                                 |
|   |       |   | PROGRAM<br>ELEMENT NO.<br>62602F   | PROJECT<br>NO.<br>2567   | TASK<br>NO.<br>03               |
|   |       |   | WORK UNIT<br>ACCESSION NO.<br>22   |  |                                 |
| 11. TITLE (Include Security Classification)<br>Aerodynamics of Missiles with Offset Fin Configurations  |       |   |  |  |                                 |
| 12. PERSONAL AUTHOR(S)<br>Gregg L. Abate, and Wayne H. Hathaway   |       |   |  |  |                                 |
| 13a. TYPE OF REPORT<br>Paper  |       | 13b. TIME COVERED<br>FROM Oct 87 to Aug 89        |  | 14. DATE OF REPORT (Year, Month, Day)<br>September 1989                              |                                 |
| 15. PAGE COUNT<br>9   |       |   |  |  |                                 |
| 16. SUPPLEMENTARY NOTATION<br>AIAA Atmospheric Flight Mechanics Symposium<br>Boston, Massachusetts - August 1989  |       |   |  |  |                                 |
| 17. COSATI CODES  |       |   | 18. SUBJECT TERMS (Continue on reverse if necessary and identify by block number)                    |  |                                 |
| FIELD   | GROUP | SUB-GROUP   | Offset Fins, Aerodynamics  |  |                                 |
|   |       |   | Missile Stability, Dynamic Stability   |  |                                 |
|   |       |   | Flexible Fins, Side Moments  |  |                                 |
| 19. ABSTRACT (Continue on reverse if necessary and identify by block number)<br>Subsonic and transonic aerodynamic data for offset fin configurations are presented. Free-flight aeroballistic tests to obtain this data were conducted at atmospheric pressure over a Mach number range of 0.6 to 1.6. The aerodynamic coefficients and derivatives presented were extracted from the position-attitude-time histories of the experimentally measured trajectories using nonlinear numerical integration data reduction routines. Results of this testing and analysis show the static and dynamic stability variations for four different fin offset configurations. The presence of a side moment dependent on pitch angle results in dynamic instability under certain conditions. The stability boundaries associated with this side moment are mapped. Designers should consider this moment whenever offset fins are utilized. |       |   |  |  |                                 |
| 20. DISTRIBUTION/AVAILABILITY OF ABSTRACT<br><input type="checkbox"/> UNCLASSIFIED/UNLIMITED <input checked="" type="checkbox"/> SAME AS RPT. <input type="checkbox"/> DTIC USERS   |       |   | 21. ABSTRACT SECURITY CLASSIFICATION<br>Unclassified   |  |                                 |
| 22a. NAME OF RESPONSIBLE INDIVIDUAL<br>Gregg L. Abate   |       |   | 22b. TELEPHONE (Include Area Code)<br>(904) 882-4085   |  | 22c. OFFICE SYMBOL<br>AFATL/FXA |

# AERODYNAMICS OF MISSILES WITH OFFSET FIN CONFIGURATIONS

Gregg L. Abate\*  
Aerodynamics Branch  
Aeromechanics Division  
Air Force Armament Laboratory  
Eglin AFB, FL

and

Wayne H. Hathaway\*\*  
Arrow Tech Associates  
Lakewood Commons  
South Burlington, VT

A-1

## Abstract

Subsonic and transonic aerodynamic data for offset fin configurations are presented. Free-flight aeroballistic tests to obtain this data were conducted at atmospheric pressure over a Mach number range of 0.6 to 1.6. The aerodynamic coefficients and derivatives presented were extracted from the position-attitude-time histories of the experimentally measured trajectories using nonlinear numerical integration data reduction routines. Results of this testing and analysis show the static and dynamic stability variations for four different fin offset configurations. The presence of an side moment dependent on pitch angle results in dynamic instability under certain conditions. The stability boundaries associated with this side moment are mapped. Designers should consider this moment whenever offset fins are utilized.

## Nomenclature

|                                |  |                                |  |
|--------------------------------|--|--------------------------------|--|
| A                              | = reference area   | $C_{N\delta}$                  | = normal force due to trim                               |
| ABARM                          | = max total angle of attack                                      | $C_{N\delta 3}, C_{N\delta 5}$ | = cubic and fifth order normal force coefficients        |
| $a_C$                          | = Coriolis acceleration  | $C_n, C_{nsm}$                 | = side moment coefficient                                |
| $C_l$                          | = roll moment coefficient  | $C_{n\alpha}$                  | = slope of side moment versus $\sin \alpha$              |
| $C_{lp}$                       | = spin decay roll moment coefficient                             | $C_{np\alpha}$                 | = Magnus moment derivative                               |
| $C_l$                          | = induced roll moment coefficient derivative                     | $C_{n\gamma\alpha}$            | = induced side moment derivative                         |
| $C_{m\alpha}$                  | = pitching moment coefficient derivative per $\sin \alpha$       | $C_{x0}$                       | = axial force coefficient at zero angle of attack        |
| $C_{m\dot{\alpha}}$            | = pitching moment coefficient derivative per $\sin \dot{\alpha}$ | $C_{x\alpha 3}$                | = squared axial force coefficient versus $\sin \alpha$   |
| $C_{mq}$                       | = pitch damping derivative                                       | $C_{xM}$                       | = slope of axial force versus Mach number                |
| $C_{m\delta}$                  | = moment due to trim   | $C_{Yp}$                       | = Magnus force coefficient                               |
| $C_{m\delta 3}, C_{m\delta 5}$ | = cubic and fifth order coefficient derivatives                  | $C_Y$                          | = side force coefficient                                 |
| $C_{mM}$                       | = slope of pitching moment versus Mach number                    | d                              | = body diameter  |
| $C_N$                          | = normal force coefficient                                       | DBSQ                           | = effective mean angle of attack squared                 |
| $C_{N\alpha}$                  | = normal force coefficient derivative per $\sin \alpha$          | g                              | = acceleration due to gravity                            |
|                                |  | $I_x, I_y$                     | = moments of inertia about the x and y axis              |
|                                |  | l, m, n                        | = aerodynamic roll, pitch, and yaw moments               |
|                                |  | $\bar{m}$                      | = model mass   |
|                                |  | M                              | = Mach number  |
|                                |  | p, q, r                        | = roll, pitch, and yaw angular velocity components       |
|                                |  | $\bar{q}$                      | = dynamic pressure                                       |
|                                |  | $\rho$                         | = air density  |
|                                |  | u, v, w                        | = missile velocity components in fixed plane coordinates |
|                                |  | V                              | = total velocity   |
|                                |  | $\alpha$                       | = total angle of attack                                  |
|                                |  | $\gamma$                       | = aerodynamic roll angle                                 |
|                                |  | $\theta, \psi, \phi$           | = missile orientation angles                             |
|                                |  | $\lambda_1, \lambda_2$         | = linear theory vector damping rates                     |
|                                |  | Superscript                    |  |
|                                |  | -                              | = total coefficient                                      |
|                                |  | .                              | = first derivative WRT time                              |

\* Aerospace Engineer, Member AIAA

\*\* Advanced Munitions Engineer, Member AIAA

## Introduction

In an effort to develop innovative missile designs, the concept of 'offset fins' has been proposed. Unlike traditional missiles with fins perpendicular to the body, offset fin configurations have fins at angles less than 90 degrees from a plane tangent to the cylindrical body at the fin interface. For tube launched applications, this provides significant advantages in packaging and design simplicity.

To better understand the aerodynamics and stability characteristics of this class of configurations, the Aerodynamics Branch of the Air Force Armament Laboratory conducted a series of free flight tests to experimentally investigate the aerodynamics.

The purpose of the research testing reported herein was to investigate four offset fin configurations of 60 deg, 45 deg, 30 deg, and 0 deg at Mach numbers ranging from 0.6 to 1.6. The test program was conducted in the Aeroballistic Research Facility (ARF), Eglin Air Force Base, Florida.

## Facilities & Test Models

### Free Flight Range

The Aeroballistic Research Facility<sup>1</sup> (ARF) is an enclosed concrete structure used to examine the exterior ballistics of various free-flight munitions. The facility contains a gun room, control room, model measurement room, blast chamber, and an instrumented range. The range atmosphere is controlled and closely monitored.

The 207 meter range has a 3.66 meter cross-section for the first 69 meters and a 4.88 meter square cross-section for the remaining length. The range has 131 locations available as instrumentation sites and each location has a physical separation of 1.52 meters. Presently 50 of these sites are used to house fully instrumented orthogonal shadowgraph stations. At each of these stations, the maximum shadowgraph window (an imaginary circle in which a projectile will cast a shadow on two orthogonal reflective screens) is 2.13 meters in diameter. The orthogonal photographs of the model's shadow can be used to determine the spatial position and angular orientation of the model at each of the 50 instrumented sites. The discrete time dynamic data of positions and orientations are then used by the data reduction program to determine the aerodynamic forces and moments acting on the model for that flight.

### Models & Test Conditions

The research configuration which is referred to as an offset fin configuration is illustrated in Figure 1. This test model is a 10-caliber ogive-cylinder-tail configuration. It has a 2.5 caliber tangent ogive, and the afterbody is a right circular cylinder 7.5 calibers in length. The fins are of a double wedge clipped delta configuration whose trailing edges fit flush with the base of the model.

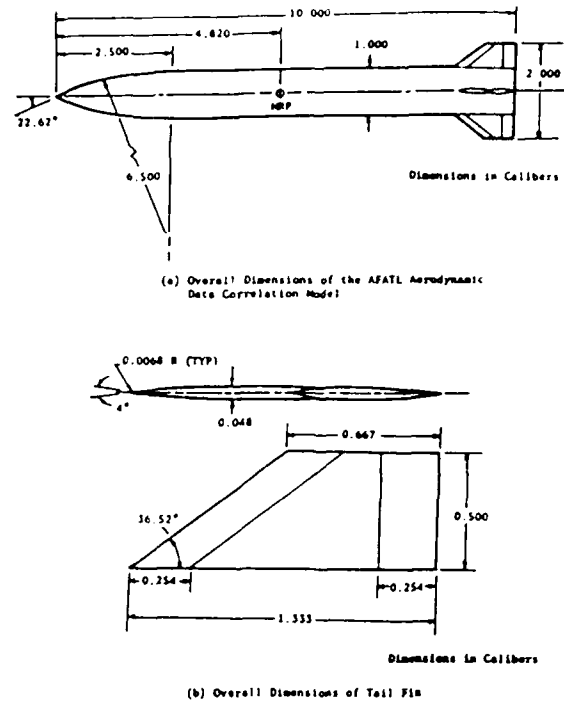


Figure 1. Air Force Basic Research Configuration (Ref. 4)

This model, with fins in the conventional 90 deg orientation, has been the subject of considerable experimental research in both wind tunnel and ballistic spark range testing. Therefore, a large pre-existing data base is available for the 90 deg offset. Reference 2 is an excellent source for both wind tunnel and range data.

Figure 2 illustrates the fin offsets which are the subject of this investigation. Table 1 summarizes the typical mass properties of the test models.

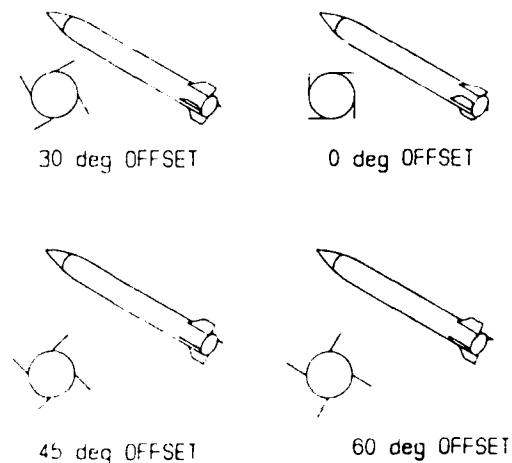


Figure 2. Offset Fin Configurations Tested

Table 1. Physical Properties

|                            | 0-degree | 30,45,60-degree |
|----------------------------|----------|-----------------|
| Diameter, cm.              | 1.91     | 1.91            |
| Mass, gm.                  | 189.0    | 127.1           |
| $I_x$ , gm-cm <sup>2</sup> | 89.2     | 63.8            |
| $I_y$ , gm-cm <sup>2</sup> | 3889     | 3889            |
| Length, cm.                | 19.1     | 19.1            |
| C.G., percent from nose    | 39.7     | 49.1            |

Roll pins were installed in each test model to acquire roll orientation data. This data is critical towards determining any aerodynamic trends as a function of roll angle (i.e. trims and induced forces and moments).

#### Data Analysis

Extraction of the aerodynamic coefficients and derivatives is the primary goal in analyzing the trajectories measured in the ARF. This is accomplished by using ARFDAS described in References 3 and 4. ARFDAS incorporates a standard linear theory analysis (References 5 and 6) and a six-degree-of-freedom (6DOF) numerical integration technique. The 6DOF routine incorporates the Maximum Likelihood Method (MLM) to match the theoretical trajectory to the experimentally measured trajectory. The MLM is an iterative procedure that adjusts the aerodynamic coefficients to maximize a likelihood function. The use of this likelihood function eliminates the inherent assumption in least squares theory that the magnitude of the measurement noise must be consistent between dynamic parameters (irrespective of units). In general, the aerodynamics can be nonlinear functions of the angle of attack, Mach number, and aerodynamic roll angle.

ARFDAS represents a complete ballistic range data reduction system capable of analyzing both symmetric and asymmetric bodies. The essential steps of the data reduction system are to: (1) assemble the dynamic range data (time, position, attitude), physical properties, and atmospheric conditions, (2) perform linear theory analysis, (3) perform 6DOF analysis for final aerodynamics. These steps have been integrated into ARFDAS to provide the test engineer with a convenient and efficient means of interaction. At each step in the analysis, permanent records for each flight are maintained such that subsequent analysis with data modifications are much faster.

Each model tested in the ARF was initially analyzed separately, then some were combined in groups for simultaneous analysis using the multiple fit capability. This provides a common set of aerodynamics that match each of the separately measured position-attitude-time profiles. The multiple fit approach provides a more complete spectrum of angle of attack and roll orientation than would be available from any one trajectory considered separately. This increases the probability that the determined coefficients define the model's aerodynamics over the entire range of trajectories.

#### Equations of Motion

The aerodynamic data presented in this paper were obtained using the fixed plane 6DOF analysis (MLMFEXPL). The equations of motion are derived with respect to a fixed plane coordinate system. The x-axis points downrange, the y-axis points to the left looking downrange, and the z-axis points up. The 6DOF differential equations of motion in this system are:

$$\dot{u} = g \sin \theta - qw + rv - a_{cu} + \frac{F_x}{m} \quad (1)$$

$$\dot{v} = -ru - r \tan \theta - a_{cv} + \frac{F_y}{m} \quad (2)$$

$$\dot{w} = -g \cos \theta + rv \tan \theta + qu - a_{cw} + \frac{F_z}{m} \quad (3)$$

$$\dot{p} = \frac{l}{I_x} \quad (4)$$

$$\dot{q} = -r^2 \tan \theta - \left(\frac{I_z}{I_y}\right) rp + \frac{m}{I_y} \quad (5)$$

$$\dot{r} = qr \tan \theta + \left(\frac{I_z}{I_y}\right) qp + \frac{n}{I_y} \quad (6)$$

Once the aerodynamic forces and moments are determined, the solution of Equations 1-6 will define the 6DOF flight motion with respect to the fixed plane coordinate system. Since the position-attitude measurements, as acquired from the ballistic spark range, are relative to the Earth-fixed coordinate system, additional transformation equations are required. Equations 7-12 are these transformation equations shown below in terms of the fixed plane Euler angles ( $\theta, \psi$ ) and the angle of rotation about the missile axis ( $\phi$ ).

$$\dot{x} = u \cos \theta \cos \psi - v \sin \psi + w \sin \theta \cos \psi \quad (7)$$

$$\dot{y} = u \cos \theta \sin \psi + v \cos \psi + w \sin \theta \sin \psi \quad (8)$$

$$\dot{z} = u \sin \theta + w \cos \theta \quad (9)$$

$$\dot{\theta} = q \quad (10)$$

$$\dot{\psi} = \frac{r}{\cos \theta} \quad (11)$$

$$\dot{\phi} = p + r \tan \theta \quad (12)$$

Coriolis accelerations ( $a_{cu}, a_{cv}, a_{cw}$ ) are also included in Equations 1-3. Equations 1-12 are numerically integrated using a fourth-order Runge-Kutta scheme.

## Aerodynamic Model

Previous testing of wraparound fins have shown instabilities in the form of an out of plane side moment ( $C_{n\alpha}$ ) leading to undamped coning motions which are highly Mach number dependent, Reference 7 contains test results from prior wraparound fin testing.

The aerodynamic coefficients and derivatives, shown in Equations 13-18, were expanded as functions of Mach number, sine of the total angle of attack, and the aerodynamic roll angle. These expansions are shown in detail in Reference 8. However, the side moment expansion was assumed to be linear (i.e.  $\bar{C}_{n\alpha} = C_{n\alpha}$ ).

The aerodynamic forces and moments are defined as follows:

$$F_x = -\bar{q}AC_x \quad (13)$$

$$F_y = \bar{q}A \left[ -\bar{C}_{N\alpha} \frac{v}{V} + \frac{pd}{2V} \bar{C}_{Yp\alpha} \frac{v}{V} + \bar{C}_{Y\gamma\alpha} \frac{v}{V} + (\bar{C}_{N\delta} \delta_A) \sin \phi - (\bar{C}_{N\delta} \delta_B) \cos \phi \right] \quad (14)$$

$$F_z = \bar{q}A \left[ -\bar{C}_{N\alpha} \frac{v}{V} - \frac{pd}{2V} \bar{C}_{Yp\alpha} \frac{v}{V} - \bar{C}_{Y\gamma\alpha} \frac{v}{V} - (\bar{C}_{N\delta} \delta_A) \sin \phi - (\bar{C}_{N\delta} \delta_B) \cos \phi \right] \quad (15)$$

$$l = \bar{q}A \left[ \frac{pd}{2V} \bar{C}_{lp} + \bar{C}_l \right] \quad (16)$$

$$m = \bar{q}Ad \left[ \bar{C}_{m\alpha} \frac{v}{V} + \frac{qd}{2V} \bar{C}_{mq} + \frac{pd}{2V} \bar{C}_{mp\alpha} \frac{v}{V} + \bar{C}_{m\gamma\alpha} \frac{v}{V} + \bar{C}_{m\alpha} \frac{v}{V} + \bar{C}_{m\delta} \delta_A \cos \phi - \bar{C}_{m\delta} \delta_B \sin \phi \right] \quad (17)$$

$$n = \bar{q}Ad \left[ -\bar{C}_{m\alpha} \frac{v}{V} + \frac{rd}{2V} \bar{C}_{mq} + \frac{pd}{2V} \bar{C}_{mp\alpha} \frac{v}{V} + \bar{C}_{m\gamma\alpha} \frac{v}{V} + \bar{C}_{m\alpha} \frac{v}{V} + \bar{C}_{m\delta} \delta_A \sin \phi + \bar{C}_{m\delta} \delta_B \cos \phi \right] \quad (18)$$

## Results

Aerodynamic force and moment coefficients have been extracted from the free flight motion data. The analysis methodology utilized includes both linear theory and 6DOF reduction. Results are presented for 0 deg, 30 deg, 45 deg, and 60 deg offset fin conditions. Where applicable, comparisons are made to results from Reference 2 which represents the same research configuration at a typical 90 deg fin orientation.

The aerodynamic coefficients and derivatives extracted from the experimentally measured trajectories are plotted in Figures 3-6 and tabulated in Table 2. These figures show the zero angle-of-attack coefficients and derivatives obtained using the fixed plane 6DOF analysis.

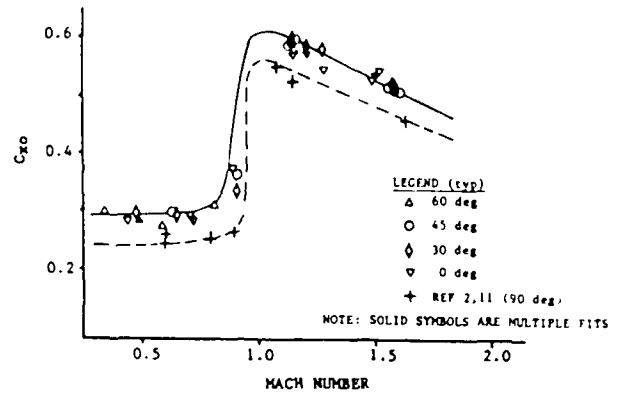


Figure 3. Zero Yaw Axial Force ( $C_{x0}$ ) versus Mach number

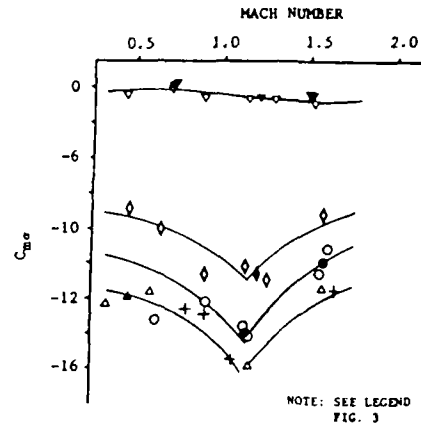


Figure 4. Pitch Moment Coefficient Derivative ( $C_{m\alpha}$ ) versus Mach Number

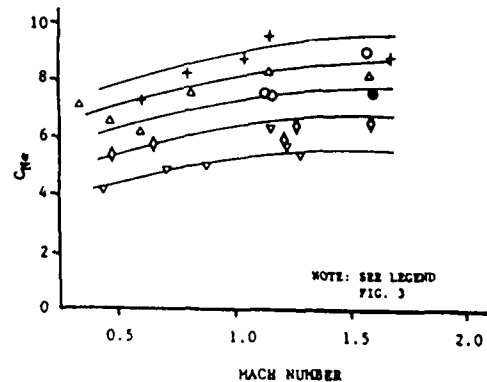


Figure 5. Normal Force Coefficient Derivative ( $C_{N\alpha}$ ) versus Mach Number

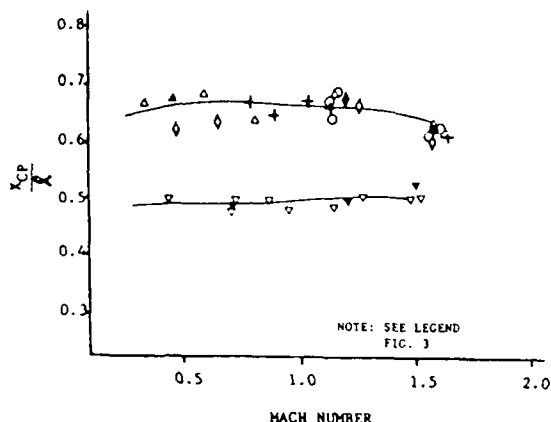


Figure 6. Center of Pressure ( $X_{cp}/l$ ) versus Mach Number

The zero yaw drag plot, Figure 3, shows little difference for the four configurations tested. There was, however, a slight overall increase in drag for these offset fin models compared to the 90 deg models (ref 2,11). The discrepancy between offset fin models and 90 deg models is not understood; however, the fact that this drag remains unchanged as a function of offset fin angle indicates there is no strong drag dependence on offset fin angle.

The pitching moment coefficient derivative results for the 0-degree fin offset configuration were converted to the same C.G. location as the other fin offsets as plotted in Figure 4. The Table 2 results are presented relative to the actual model C.G. as measured. This figure indicates that there is little difference in stability between the 90 deg and 60 deg fin offset models. As fin offset angle is increased there is a steady decrease in stability to the 45 deg and 30 deg models. Then, there is a large decrease in stability from 30 deg to 0 deg. This indicates that fin effectiveness is decreasing slowly near 90 deg fin offsets followed by a sharp decrease somewhere between 30 deg and 0 deg. The normal force derivatives, Figure 5, however, show a steady decrease as a function of offset fin angle. It is also of interest to note that the data shown in Figure 6 illustrates that much of the loss in static stability for the 0 deg fin offset configuration comes from a rather dramatic forward shift of the center-of-pressure.

Figures 7-10 contain representative motion plots for each fin offset. Note the indications of dynamic instability for the 0 deg and 30 deg offsets. Based on prior research with wraparound fin configurations, the presence of out of plane moments and roll resonance conditions could be expected. The out of plane moments (side moment) could be due to; (1) the induced side moment based on the roll orientation relative to the cross-flow velocity component ( $\bar{C}_{ny\alpha}$  - Table 4), or (2) the moment as a function of pitch angle ( $\bar{C}_{n\alpha}$  - Table 4).

In matching the observed motion, the dominant side moment was  $C_{n\alpha}$ . The inclusion of this aerodynamic coefficient during the data reduction process made a dramatic improvement to the quality of the fits. This was most significant for the 0 deg and 30 deg fin offsets. The trim angles were on the order of 0.5 degree and for those flights near resonance, explained the damping trends of the observed motions.

## Discussion

### Dynamic Stability

The resulting aerodynamic force and moment coefficients show nonlinear trends as a function of Mach number, angle of attack, and aerodynamic roll angle.

The inclusion of the side moment due to pitch angle,  $C_{n\alpha}$ , was critical in order to adequately fit the measured motion patterns. The tendency of the motion to develop into a circular pattern provides a clue to the possible effects of this side moment. Both Murphy<sup>5</sup> and Nicolaides<sup>6</sup> have studied the consequences of a side moment due to pitch on the dynamic stability of a finned missile. The equations for the computation of the nutational and precessional damping rates with  $C_{n\alpha}$  included are as follows:

$$\lambda_1 = \frac{\rho A}{4\pi} \left[ -C_{N\alpha} \left( 1 - \frac{1}{0} \right) + (C_{mq} + C_{m\alpha}) \left( \frac{\bar{m} \alpha^2}{2I_y} \right) \left( 1 + \frac{1}{0} \right) + \left( \frac{\bar{m} \alpha^2}{I_y} \right) \left( \frac{1}{0} \right) C_{N\alpha} \left( \frac{2V}{\bar{p} \alpha} \right) \right] \quad (19)$$

$$\lambda_2 = \frac{\rho A}{4\pi} \left[ -C_{N\alpha} \left( 1 + \frac{1}{0} \right) + (C_{mq} + C_{m\alpha}) \left( \frac{\bar{m} \alpha^2}{2I_y} \right) \left( 1 - \frac{1}{0} \right) - \left( \frac{\bar{m} \alpha^2}{I_y} \right) \left( \frac{1}{0} \right) C_{N\alpha} \left( \frac{2V}{\bar{p} \alpha} \right) \right] \quad (20)$$

where:

$$0 = \sqrt{1 - \frac{I}{I_y}} \quad (21)$$

$$S_i = \frac{2I_y^2 p^2}{\pi \rho I_y C_{m\alpha} d^3 V^2} \quad (22)$$

Equations 19-20 assume that the Magnus moment is negligible. By computing the required side moment coefficient,  $C_{n\alpha}$ , for  $\lambda$  equal to zero will determine the dynamic stability boundary. This was done and the results are plotted in Figure 11 for the 0 deg and 30 deg fin offsets. The plots include Mach numbers of 0.7, 1.2, and 1.5/1.6. This shows that based on the determined side moment coefficients, a dynamic instability exists due to this moment, subsonically for these fin offsets.

Table 2. 6 DDF Aerodynamics

| Single Fits   |             |            |            |               |                |               |               |                 |                 |            |          |          |                |            |
|---------------|-------------|------------|------------|---------------|----------------|---------------|---------------|-----------------|-----------------|------------|----------|----------|----------------|------------|
| Config        | Mach Number | DBSQ ABARM | CX CX2     | CNa CNa5      | Cma Cma3       | Cmq Cmq2      | CZga3 CNa3    | CYga3 CNa3      | Clga2 Cmsm      | Clp Clp    | Cma CmaB | Cma CmaB | Probable Error |            |
|               |             |            |            |               |                |               |               |                 |                 |            |          |          | X(m)           | Angle(deg) |
|               |             |            |            |               |                |               |               |                 |                 |            |          |          | Y-Z(m)         | Roll(deg)  |
| 60 Deg        | 0.335       | 34.4       | 0.298      | 7.02          | -12.269        | -416.0        | 0.0           | 0.0             | 0.00            | -2.000     | 0.041    | -0.015   | 0.0013         | 0.286      |
|               |             | 9.9        | 0.750      | 0.00          | 0.00           | 0.0           | 0.0           | 0.0             | 0.95            | 0.016      | 0.022    | 0.091    | 0.0007         | 8.913      |
| 60 Deg        | 0.594       | 22.8       | 0.275      | 6.12          | -11.564        | -333.3        | 0.0           | 0.0             | 0.00            | -2.000     | 0.000    | -0.152   | 0.0010         | 0.176      |
|               |             | 9.2        | 0.750      | 0.00          | 0.00           | 0.0           | 0.0           | 0.0             | 0.51            | -0.005     | 0.000    | 0.016    | 0.0012         | 2.813      |
| 60 Deg        | 0.813       | 0.5        | 0.310      | 7.50          | -11.030        | -345.2        | 0.0           | 0.0             | 0.00            | -2.931     | 0.000    | 0.050    | 0.0023         | 0.144      |
|               |             | 1.3        | 0.750      | 0.00          | 0.00           | 0.0           | 0.0           | 0.0             | 1.13            | -0.052     | 0.000    | 0.086    | 0.0026         | 9.197      |
| 60 Deg        | 1.160       | 1.8        | 0.579      | 8.25          | -15.805        | -292.1        | 0.0           | 0.0             | 0.00            | -2.000     | 0.000    | 0.020    | 0.0019         | 0.162      |
|               |             | 4.5        | 0.750      | 0.00          | 0.00           | 0.0           | 0.0           | 0.0             | 0.00            | -0.007     | 0.000    | 0.004    | 0.0025         | 5.149      |
| 60 Deg        | 1.585       | 3.2        | 0.524      | 8.10          | -11.280        | -382.3        | 0.0           | 0.0             | 0.00            | -2.000     | 0.000    | 0.018    | 0.0023         | 0.160      |
|               |             | 5.4        | 0.750      | 0.00          | 0.00           | 0.0           | 0.0           | 0.0             | 0.00            | -0.010     | 0.000    | 0.046    | 0.0024         | 14.740     |
| 45 Deg        | 0.628       | 5.4        | 0.298      | 7.00          | -13.225        | -250.0        | 423.0         | -543.1          | 0.00            | -4.291     | 0.037    | -0.016   | 0.0020         | 0.389      |
|               |             | 4.2        | 0.750      | 0.00          | 0.00           | 0.0           | -981.7        | 462.3           | -0.30           | -0.010     | 0.034    | 0.085    | 0.0026         | 11.000     |
| 45 Deg        | 0.912       | 0.2        | 0.362      | 7.00          | -12.139        | -126.1        | 0.0           | 0.0             | 0.00            | -2.124     | 0.000    | -0.080   | 0.0030         | 0.194      |
|               |             | 0.9        | 0.750      | 0.00          | 0.00           | 0.0           | 0.0           | 0.0             | 0.00            | -0.083     | 0.000    | -0.083   | 0.0021         | 19.630     |
| 45 Deg        | 1.133       | 0.1        | 0.590      | 7.59          | -13.614        | -152.5        | 0.0           | 0.0             | 0.00            | -2.512     | 0.000    | -0.016   | 0.0021         | 0.113      |
|               |             | 0.8        | 0.750      | 0.00          | 0.00           | 0.0           | 0.0           | 0.0             | 0.00            | 0.030      | 0.000    | -0.026   | 0.0026         | 7.591      |
| 45 Deg        | 1.153       | 3.8        | 0.598      | 7.30          | -14.113        | -264.8        | 0.0           | 0.0             | 0.00            | -2.000     | 0.000    | 0.053    | 0.0028         | 0.205      |
|               |             | 5.6        | 0.750      | 0.00          | 0.00           | 0.0           | 0.0           | 0.0             | 0.00            | 0.008      | 0.000    | -0.023   | 0.0023         | 21.150     |
| 45 Deg        | 1.571       | 1.4        | 0.517      | 8.96          | -10.535        | -436.2        | 0.0           | 0.0             | 0.00            | -2.000     | 0.000    | 0.074    | 0.0027         | 0.270      |
|               |             | 3.0        | 0.750      | 0.00          | 0.00           | 0.0           | 0.0           | 0.0             | 0.00            | 0.010      | 0.000    | -0.008   | 0.0023         | 4.965      |
| 45 Deg        | 1.612       | 0.6        | 0.509      | 6.98          | -9.130         | -250.0        | 0.0           | 0.0             | 0.00            | -2.000     | 0.000    | 0.014    | 0.0012         | 0.186      |
|               |             | 2.1        | 0.750      | 0.00          | 0.00           | 0.0           | 0.0           | 0.0             | 0.00            | 0.002      | 0.000    | -0.017   | 0.0026         | 10.180     |
| 30 Deg        | 0.470       | 6.2        | 0.296      | 5.32          | -6.897         | -250.0        | 0.0           | 0.0             | 0.00            | -2.000     | 0.000    | -0.075   | 0.0006         | 0.323      |
|               |             | 4.5        | 0.750      | 0.00          | 0.00           | 0.0           | 0.0           | 0.0             | -1.43           | -0.005     | 0.000    | -0.082   | 0.0017         | 3.181      |
| 30 Deg        | 0.650       | 101.6      | 0.296      | 5.32          | -8.045         | -176.2        | 0.0           | 0.0             | 0.00            | -31.349    | 0.000    | 0.118    | 0.0020         | 0.602      |
|               |             | 18.2       | 0.750      | 11.6          | -16.65         | 0.0           | 0.0           | 0.0             | -0.65           | -0.103     | 0.000    | 0.063    | 0.0022         | 11.360     |
| 30 Deg        | 0.911       | 1.7        | 0.335      | 7.00          | -10.601        | -200.6        | 0.0           | 0.0             | 0.00            | -1.863     | 0.000    | -0.112   | 0.0028         | 0.224      |
|               |             | 2.2        | 0.750      | 0.00          | 0.00           | 0.0           | 0.0           | 0.0             | -1.41           | -0.043     | 0.000    | -0.030   | 0.0020         | 11.880     |
| 30 Deg        | 1.138       | 0.6        | 0.595      | 8.00          | -10.197        | -250.0        | 0.0           | 0.0             | 0.00            | -2.000     | 0.000    | 0.010    | 0.0021         | 0.193      |
|               |             | 2.4        | 0.750      | 0.00          | 0.00           | 0.0           | 0.0           | 0.0             | 0.00            | 0.003      | 0.000    | -0.005   | 0.0025         | 35.150     |
| 30 Deg        | 1.262       | 21.5       | 0.577      | 6.29          | -10.975        | -200.0        | 0.0           | 0.0             | 0.00            | -10.330    | 0.000    | 0.080    | 0.0031         | 0.531      |
|               |             | 7.9        | 0.750      | 0.00          | 0.00           | 0.0           | 0.0           | 0.0             | -0.74           | -0.028     | 0.000    | 0.052    | 0.0029         | 7.616      |
| 30 Deg        | 1.578       | 5.2        | 0.520      | 6.43          | -7.122         | -357.5        | 0.0           | 0.0             | 0.00            | -5.426     | 0.000    | 0.038    | 0.0023         | 0.224      |
|               |             | 5.7        | 0.750      | 0.00          | 0.00           | 0.0           | 0.0           | 0.0             | -0.55           | -0.045     | 0.000    | 0.024    | 0.0024         | 9.148      |
| 0 Deg         | 0.442       | 323.4      | 0.281      | 4.16          | -3.933         | -288.6        | 0.0           | 0.0             | 0.00            | -9.414     | 0.000    | -0.020   | 0.0019         | 0.392      |
|               |             | 30.1       | 1.000      | 13.55         | -47.13         | 0.0           | 0.0           | 0.0             | -2.17           | -0.101     | 0.000    | -0.036   | 0.0014         | 15.780     |
| 0 Deg         | 0.705       | 133.8      | 0.292      | 4.84          | -3.713         | -100.0        | 0.0           | 0.0             | 0.00            | 0.924      | 0.000    | 0.058    | 0.0013         | 0.417      |
|               |             | 21.4       | 0.833      | 0.00          | -38.89         | 0.0           | 0.0           | 0.0             | -1.55           | -0.021     | 0.000    | 0.002    | 0.0014         | 10.660     |
| 0 Deg         | 0.725       | 341.1      | 0.283      | 3.32          | -3.348         | -106.8        | 0.0           | 0.0             | 0.00            | -5.392     | 0.037    | -0.025   | 0.0028         | 0.695      |
|               |             | 33.5       | 1.000      | 17.07         | -48.95         | 0.0           | 0.0           | 0.0             | -1.71           | -0.050     | -0.039   | -0.011   | 0.0022         | 16.170     |
| 0 Deg         | 0.884       | 221.5      | 0.375      | 5.06          | -5.091         | -100.0        | 0.0           | 0.0             | 0.00            | 3.667      | 0.000    | -0.060   | 0.0020         | 0.644      |
|               |             | 34.1       | 0.470      | 13.16         | -76.32         | 0.0           | 0.0           | 0.0             | -2.52           | -0.018     | 0.000    | -0.126   | 0.0012         | 9.836      |
| 0 Deg         | 1.147       | 117.8      | 0.573      | 6.29          | -5.600         | -253.5        | 0.0           | 0.0             | 0.00            | -6.700     | 0.000    | 0.450    | 0.0026         | 0.497      |
|               |             | 18.4       | 1.964      | 0.00          | -51.77         | 0.0           | 0.0           | 0.0             | -0.34           | -0.064     | 0.000    | -0.089   | 0.0026         | 14.500     |
| 0 Deg         | 1.280       | 15.0       | 0.542      | 5.38          | -5.625         | -244.8        | 0.0           | 0.0             | 0.00            | 0.680      | 0.000    | -0.017   | 0.0028         | 0.305      |
|               |             | 7.7        | 7.473      | 0.00          | -35.87         | 0.0           | 0.0           | 0.0             | -0.25           | 0.004      | 0.000    | -0.013   | 0.0022         | 4.773      |
| 0 Deg         | 1.491       | 26.7       | 0.527      | 4.55          | -4.500         | -100.0        | 57.4          | -33.8           | 0.00            | -1.000     | 0.000    | -0.029   | 0.0026         | 0.351      |
|               |             | 9.9        | 3.500      | 0.00          | -53.63         | 0.0           | 27.1          | 64.5            | -0.47           | -0.005     | 0.000    | 0.042    | 0.0014         | 5.879      |
| 0 Deg         | 1.523       | 50.8       | 0.546      | 4.70          | -5.039         | -109.7        | 33.9          | 137.5           | 0.00            | -1.000     | -0.021   | -0.074   | 0.0026         | 0.576      |
|               |             | 9.6        | 2.000      | 0.00          | -10.04         | 0.0           | 0.0           | 0.0             | -0.25           | -0.012     | -0.065   | -0.161   | 0.0018         | 11.400     |
| Multiple fits |             |            |            |               |                |               |               |                 |                 |            |          |          |                |            |
| Config        | Mach Number | DBSQ ABARM | CX CX2 CX4 | CNa CNa3 CNa5 | CYpa CNa3 CNa5 | Cma Cma3 Cma5 | Cmq Cmq2 Cmq4 | CZga3 CNa3 CNa5 | CYga3 CNa3 CNa5 | Clga2 Cmsm | Clp Clp  | Cma CmaB | Probable Error |            |
|               |             |            |            |               |                |               |               |                 |                 |            |          |          | X(m)           | Angle(deg) |
|               |             |            |            |               |                |               |               |                 |                 |            |          |          | Y-Z(m)         | Roll(deg)  |
| 60 Deg        | 0.464       | 29.2       | 0.286      | 6.53          | 0.00           | -11.913       | -345.3        | 0.0             | 0.0             | 0.00       | -0.11    |          | 0.0012         | 0.276      |
|               |             | 9.7        | 0.750      | 0.00          | 0.00           | 0.000         | 0.0           | 0.0             | 0.0             | 0.00       | 0.00     |          | 0.0010         | 6.269      |
|               |             |            | 0.000      | 0.00          | 0.00           | 0.000         | 0.0           | 0.0             | 0.0             | -2.00      | 0.69     |          |                |            |
| 45 Deg        | 1.143       | 2.8        | 0.590      | 9.51          | 0.00           | -13.891       | -90.5         | 0.0             | 0.0             | 0.00       | -0.07    |          | 0.0031         | 0.241      |
|               |             | 5.1        | 0.750      | 0.00          | 0.00           | 0.000         | 0.0           | 0.0             | 0.0             | 0.00       | 0.00     |          | 0.0026         | 19.700     |
|               |             |            | 0.000      | 0.00          | 0.00           | 0.000         | 0.0           | 0.0             | 0.0             | -2.00      | 0.00     |          |                |            |
| 45 Deg        | 1.592       | 1.0        | 0.513      | 7.51          | 0.00           | -9.938        | -577.7        | 0.0             | 0.0             | 0.00       | -0.18    |          | 0.0020         | 0.223      |
|               |             | 2.9        | 0.750      | 0.00          | 0.00           | 0.000         | 0.0           | 0.0             | 0.0             | 0.00       | 0.00     |          | 0.0024         | 7.930      |
|               |             |            | 0.000      | 0.00          | 0.00           | 0.000         | 0.0           | 0.0             | 0.0             | -2.00      | -1.09    |          |                |            |
| 30 Deg        | 1.200       | 10.7       | 0.589      | 5.90          | 0.00           | -10.867       | -200.0        | 0.0             | 0.0             | 0.00       | -0.10    |          | 0.0028         | 0.419      |
|               |             | 8.0        | 0.750      | 0.00          | 0.00           | 0.000         | 0.0           | 0.0             | 0.0             | 0.00       | 1.81     |          | 0.0028         | 29.520     |
|               |             |            | 0.000      | 0.00          | 0.00           | 0.000         | 0.0           | 0.0             | 0.0             | -3.34      | -0.76    |          |                |            |
| 0 Deg         | 0.715       | 240.4      | 0.295      | 3.67          | 0.00           | -3.380        | -17.2         | 0.0             | 0.0             | 0.00       | 0.00     |          | 0.0027         | 0.624      |
|               |             | 33.4       | 1.000      | 15.39         | 0.00           | -50.797       | 0.0           | 0.0             | 0.0             | 0.00       | 0.00     |          | 0.0019         | 13.550     |
|               |             |            | 0.000      | 0.00          | 0.00           | 92.159        | 0.0           | 0.0             | 0.0             | 0.00       | -1.48    |          |                |            |
| 0 Deg         | 1.213       | 67.0       | 0.575      | 5.66          | 0.00           | -5.535        | -245.4        | 0.0             | 0.0             | 0.00       | -0.20    |          | 0.0029         | 0.393      |
|               |             | 19.0       | 2.194      | 8.30          | 0.00           | -52.871       | 0.0           | 0.0             | 0.0             | 0.00       | 0.00     |          | 0.0023         | 10.190     |
|               |             |            | -9.705     | 0.00          | 0.00           | 277.160       | 0.0           | 0.0             | 0.0             | 0.00       | -0.29    |          |                |            |
| 0 Deg         | 1.507       | 39.1       | 0.533      | 3.40          | 0.00           | -4.484        | -109.7        | 46.2            | 13.3            | 0.00       | -0.05    |          | 0.0028         | 0.470      |
|               |             | 9.9        | 2.702      | 102.21        | 0.00           | -41.095       | 0.0           | 6.1             | 57.2            | 0.00       | 0.00     |          | 0.0016         | 9.075      |
|               |             |            | 0.000      | 0.00          | 0.00           | 0.000         | 0.0           | 0.0             | 0.0             | -1.00      | -0.32    |          |                |            |

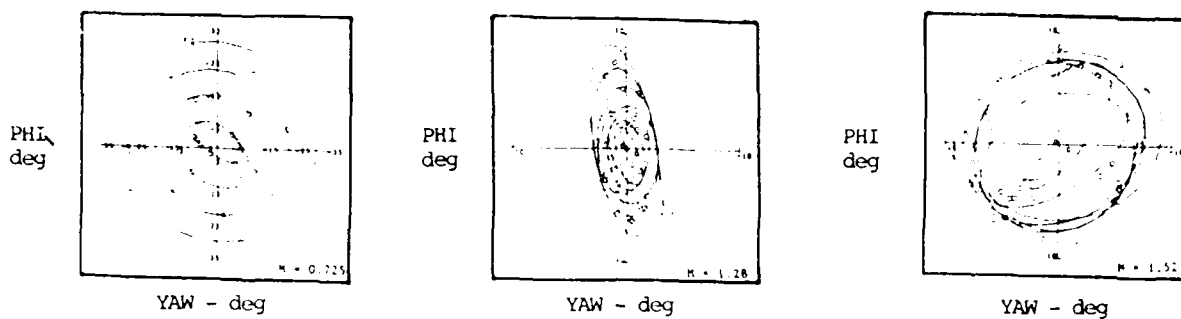


Figure 7. Motion Pattern for 0 deg Offset

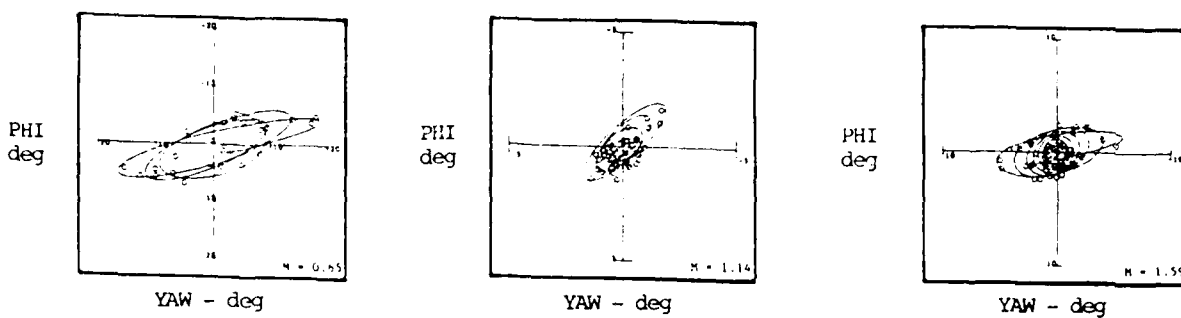


Figure 8. Motion Pattern for 30 deg Offset

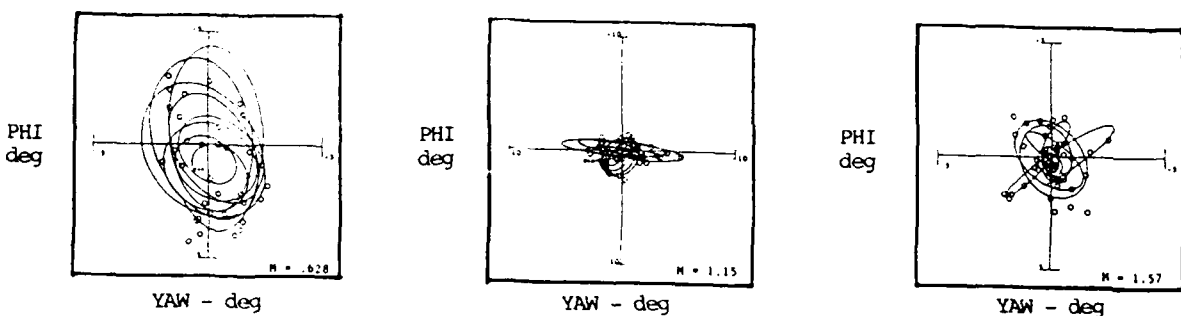


Figure 9. Motion Pattern for 45 deg Offset

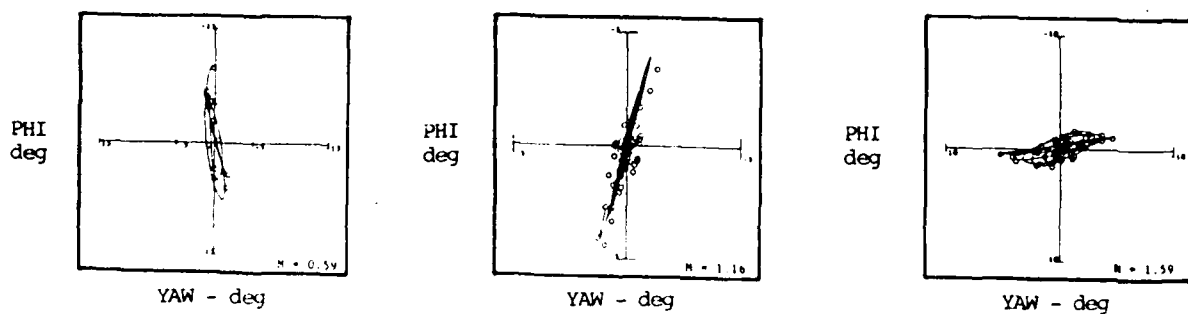


Figure 10. Motion Pattern for 60 deg Offset



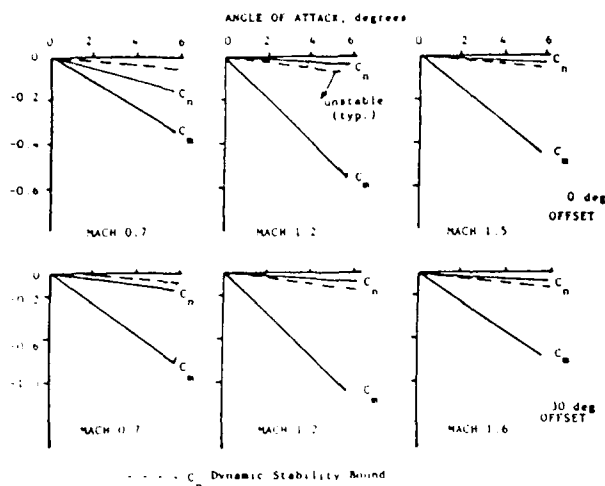
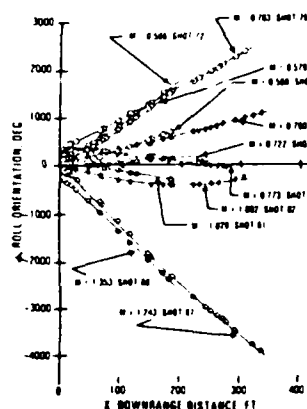


Figure 11. Stability Bounds

### Roll

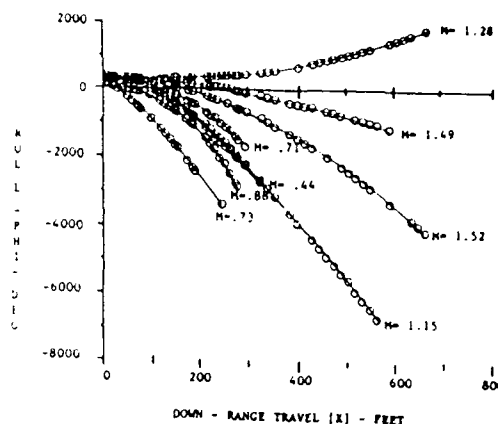
There was no attempt to control spin rate for these tests. Since trim moments were determined to exist, a roll resonance condition or amplification of the trim was of concern. A combined roll resonance and side moment affect on a given flight can create such dynamic instability as to make it difficult to accurately distinguish between the two separable aerodynamic moments during the reduction process.

Previous testing on Wrap-Around Fin configurations (Ref. 7 & 10) has shown a roll dependency due to Mach number. This is shown in Figure 12 a. Here, models tested subsonically rolled in the direction of fin curvature and model tested supersonically rolled opposite the direction of fin curvature. Figure 12 b shows the roll profiles of the 0 deg offset fin configurations. These profiles indicate that there is no roll dependence due to Mach number for these offset fin configurations.



a. Wrap-Around Fin  
(Ref 7, Fig. 8)

Figure 12. Roll vs. Mach Number



b. Present Offset Fin  
(0 deg Offset)

Figure 12. (continued) Roll vs. Mach Number

### Conclusions

Aerodynamic and stability characteristics have been determined for four offset fin configurations.

The following summarizes the important aerodynamic characteristics:

- The change in zero yaw drag is small as the fin offset angle is varied.
- The decrease in static stability is very rapid for fin offsets below 45 deg. However, static stability is insensitive to offset fin angles of 60 deg and above.
- Dynamic instabilities due to the side moment exist subsonically for the 0 deg and 30 deg offsets. There were no indications that a destabilizing side moment existed for offset fin angles of 60 deg.
- At best, large limit cycles can be expected at fin offsets less than 45 deg due to a combination of side moment and trim moment.
- There is no roll dependence of these offset fin configurations due to Mach number.

Future research should include a more controlled spin rate environment for the tests. This will allow better isolation of the roll induced side moment, the side moment due to pitch angle, and trim moment amplification due to the spin rate approaching resonance.

### References

- (1) Kittyle, R.L., Packard, J.D., and Winchenbach, G.L., "Description and Capabilities Of Aeroballistic Research Facility," AFATL-TR-87-08, May 1987.
- (2) West, K.O. and Whyte R.H., "Free Flight and Wind Tunnel Test of a Missile Configuration at Subsonic and Transonic Mach Numbers with

Angles of Attack up to 30 Degrees," Paper 39,  
11th Navy Symposium on Aeroballistics, Tevose,  
PA, August 1978.

(3) Hathaway, W., "Free Flight Data Analysis  
Using Maximum Likelihood Technique," Paper 545,  
Presented at the 28th meeting of the  
Aeroballistic Range Association, September 1977.

(4) Fischer, M., et. al., "Aeroballistic  
Facility Data Analysis System," AFATL-TR-88-48,  
September 1988.

(5) Murphy, C.H., "Free Flight Motion of  
Symmetric Missiles," BRL Report 1216, July 1963.

(6) Murphy, C.H., "Data Reduction for the  
Free Flight Spark Ranges," BRL Report 900,  
February 1954.

(7) Winchenbach, G., Buff, R., Whyte, R.,  
Hathaway, W., "Subsonic and Transonic  
Aerodynamics of a Wraparound Fin Configuration,"  
Journal of Guidance, Vol. 9, Nov-Dec 1986, pp. 627-  
632.

(8) Whyte, R. and Winchenbach, G. and Hathaway,  
W., "Subsonic Free Flight Data for a Complex  
Asymmetric Missile," Journal of Guidance,  
Control, and Dynamics, Vol. 4, Jan-Feb 1981, pp  
59-65.

(9) Nicolaidis, J., "Free Flight Dynamics,"  
University of Notre Dame, South Bend, IN, 1968.

(10) Kim, Y. and Winchenbach, G., "The Roll  
Motion of a Wraparound Fin Configuration at  
Subsonic and Transonic Mach Numbers," ALAA Paper  
85-1777, Aug. 1985.

(11) Kidd, J., "An Investigation of Drag  
Reduction Using Stepped Afterbodies," ALAA Paper  
Presented at the 27th Aerospace Sciences Meeting,  
January 1989.